ARTICLE

Hydrodeoxygenation of Anisole over Ni/α-Al_2O_3 Catalyst

Wen-wu Tang[a,c], Xing-hua Zhang[b,c*], Qi Zhang[b,c], Tie-jun Wang[b,c], Long-long Ma[b,c*]

a. Department of Chemistry, University of Science and Technology of China, Hefei 230026, China
b. Key Laboratory of Renewable Energy, Chinese Academy of Sciences, Guangzhou 510640, China
c. Guangzhou Institute of Energy Conversion, Chinese Academy of Sciences, Guangzhou 510640, China

(Dated: Received on March 30, 2016; Accepted on April 22, 2016)

Ni-based catalysts supported on different supports (α-Al_2O_3, γ-Al_2O_3, SiO_2, TiO_2, and ZrO_2) were prepared by impregnation. Effects of supports on catalytic performance were tested using hydrodeoxygenation reaction (HDO) of anisole as model reaction. Ni/α-Al_2O_3 was found to be the highest active catalyst for HDO of anisole. Under the optimal conditions, the anisole conversion is 93.25% and the hydrocarbon yield is 90.47%. Catalyst characterization using H_2-TPD method demonstrates that Ni/α-Al_2O_3 catalyst possesses more amount of active metal Ni than those of other investigated catalysts, which can enhance the catalytic activity for hydrogenation. Furthermore, it is found that the Ni/α-Al_2O_3 catalyst has excellent repeatability, and the carbon deposited on the surface of catalyst is negligible.

Key words: Anisole, Hydrodeoxygenation, Ni/α-Al_2O_3, Hydrocarbons

I. INTRODUCTION

Lignin, a three-dimensional amorphous polymer consisting of methoxylated phenylpropane structures, is contained in plant biomass with high proportion [1−3]. It can be transformed into phenolic compounds via depolymerization [4, 5]. It has been reported that yield of 13.2% phenolic monomers was obtained from organosolv pine lignin via catalytic depolymerization in the presence of MgO and THF [6]. However, obtained phenolic products were complex mixtures with high oxygen content [7, 8]. The high oxygen content led to many undesirable properties, such as high viscosity, thermal instability, corrosiveness, poor heating value and immiscibility with hydrocarbon fuels [9, 10]. Hence, the removal of oxygen is required to obtain hydrocarbons as high-graded fuels.

Hydrodeoxygenation (HDO) is an effective method for the production of hydrocarbons from lignin-derived phenolic compounds [11−13]. Bifunctional catalyst comprised by active metal and solid acid exhibits excellent activity for HDO reaction. For example, guaiacol was completely converted with high selectivity for cyclohexane over Ni/SiO_2-ZrO_2 catalyst [10]. Normally, it is considered that the metal Ni acts as hydrogenation activity center while the support SiO_2-ZrO_2 provides acidic sites for the HDO reaction.

Support material is a crucial factor determining the catalytic performance. In the past years, γ-Al_2O_3 was widely used as catalyst support for HDO catalyst due to its cheap cost, excellent texture, and suitable acidity. For example, the HDO of guaiacol with conversion of 100% and yield of 88% of cyclohexane was obtained over the Pd-based catalyst supported on γ-Al_2O_3 [14]. Oxygen contained in phenolics was also efficiently removed by hydrodeoxygenation with the sulfided NiMo/γ-Al_2O_3 and CoMo/γ-Al_2O_3 catalysts [7, 15]. However, large amount of coke formed and deposited on the surface of the catalyst during the HDO reaction process [7, 15]. Worse, partial γ-Al_2O_3 can be transformed into boehmite under hydrothermal conditions, resulting in a decrease for catalytic activity [16]. To overcome these drawbacks, many support materials such as SiO_2 [17], TiO_2 [18], and ZrO_2 [15] were also explored in the past years, exhibiting impressive catalytic activity for HDO reaction.

α-Al_2O_3 is a type of mesoporous material with excellent hydrothermal stability. However, scarce work has been done to remove oxygen from phenolics with the HDO catalyst supported on α-Al_2O_3. In this work, HDO reaction of anisole with the Ni-based catalyst supported on α-Al_2O_3 was investigated to explore the effect of support on the catalytic properties. For comparison, the Ni-based catalysts supported on γ-Al_2O_3, SiO_2, TiO_2, and ZrO_2 were also investigated in the HDO reaction of anisole.

II. EXPERIMENTS

A. Catalyst preparation

SiO_2 was prepared by chemical precipitation using NH_4NO_3 and Na_2SiO_3 as materials. The precipitate was dried at 120 °C overnight and then calcinated at

*Authors to whom correspondence should be addressed. E-mail: zhangxh@ms.giec.ac.cn, mall@ms.giec.ac.cn, Tel.: +86-20-87057673, FAX: +86-20-87057789

500 °C for 4 h. Similarly, ZrO_2 was prepared by chemical precipitation using $NH_3{\cdot}H_2O$ and $ZrOCl_2$ as material. TiO_2 was prepared by hydrolysis of $TiCl_4$. In addition, support materials α-Al_2O_3 and γ-Al_2O_3 were purchased from Aladdin Industrial Co. Ltd.

Catalysts Ni/α-Al_2O_3, Ni/γ-Al_2O_3, Ni/SiO_2, Ni/TiO_2 and Ni/ZrO_2 with 10 wt% Ni loadings were prepared by wet impregnation using $Ni(NO_3)_2{\cdot}6H_2O$ as nickel precursor. Firstly, supporting material dipped into the nickel nitrate solution. Then the solution was heated with continuous stir until water was evaporated to dryness. The obtained residues were dried at 120 °C overnight and calcinated at 500 °C for 4 h. The prepared catalyst was crushed into powder with sizes of 100−200 mesh.

The prepared catalyst Ni/α-Al_2O_3 was reduced at 700 °C while the other catalysts were reduced at 550 °C for 5 h in H_2 atmosphere before using.

B. Catalyst characterization

Brunauer-Emmett-Teller (BET) surface area (S_{BET}), average pore diameter, and pore volume of the catalyst were measured by N_2 isothermal (−196 °C) physisorption through Autosorb-iQ-2 (Qudrasorb SI, Quantachrome Instruments). The catalyst was degassed for 12 h at 250 °C under vacuum condition before N_2 adsorption.

H_2-temperature programmed reduction (H_2-TPR), NH_3-temperature programmed desorption (NH_3-TPD), and H_2-temperature programmed desorption (H_2-TPD) measurements were carried out on an automatic chemical adsorption instrument (CBP-1, Quantachrome Instruments) equipped with a thermal conductivity detector. Dispersity of Ni over different supports was calculated with the following formula:

$$D = \frac{\text{Mole of adsorbed hydrogen}}{\text{Total moles of Ni in the catalyst}} \quad (1)$$

X-ray diffraction (XRD) analysis of catalyst was carried out on an equipment (PANalytical, Netherlands) with Cu Kα (λ=0.154 nm) radiation. X-ray photoelectron spectroscopy (XPS) analysis of the catalyst was performed on the instrument of Thermo Scientific ESCALAB 250XI using A1 Kα1, 2 radiation as spectra excitation. Thermogravimetry (TG) analysis of the used catalyst was carried out under a flow of air (50 mL/min) on a thermal analyzer (TGA Q50, US). The heating rate is 15 K/min. Transmission electron microscope (TEM) profiles were obtained on a JEM-2100F (JEOL, Japan) instrument equipped with an EDX spectrometer.

C. Catalytic activity test

HDO process of anisole was carried out in a 50 mL stainless steel autoclave equipped with electric mechanical agitator. For each run, catalyst (0.5 g), solvent *n*-octane (21.5 mL) and anisole were loaded into the autoclave. 5.0 MPa H_2 was pressured into the reactor after displacing the air. The reactor was heated to a desired reaction temperature while the reagents were stirred at a rate of 800 r/min. Liquid product was collected for subsequent analysis when the reaction was completed.

D. Products analysis

Liquid products obtained from the HDO of anisole were analyzed by gas chromatography (Shimadzu GC-2010 with a FID detector and a DB-5 column) and GC-MS (Agilent 7890A-5975C with DB-FFAP capillary column). The carrier gas was He (99.995% purity), and the oven temperature program increased from 50 °C (holding for 1 min) to 260 °C (holding for 10 min) at a rate of 10 °C/min.

Anisole conversion (C) and hydrocarbon yield (Y_h) were determined with the following equation:

$$C = \frac{\text{Mole(anisole)}_{\text{initial}} - \text{Mole(anisole)}_{\text{end}}}{\text{Mole(anisole)}_{\text{initial}}} \quad (2)$$

$$Y_h = \frac{\text{Mole of hydrocarbons}}{\text{Initial mole of anisole}} \quad (3)$$

III. RESULTS AND DISCUSSION

A. Catalyst characterization

The parameters of the catalysts are shown in Table I and the structures are in Fig.S1 (supplementary materials). It was found that all tested catalysts were mesoporous materials. Their average pore diameter is in the range of 7−29 nm, and the most probable pore diameter is in the range of 3−60 nm. Among the investigated catalysts, the average pore diameter and the most probable pore diameter of Ni/α-Al_2O_3 catalyst were the smallest. They were 7.3 and 3.9 nm, respectively. In addition, TEM image of the Ni/α-Al_2O_3 catalyst was presented in Fig.S2 (supplementary material). It can be clearly seen that the metal Ni was well dispersed on the surface of α-Al_2O_3. The size of Ni particle is about 30−40 nm.

XRD profiles of different catalysts are shown in Fig.1. The weak and broad characteristic peaks centered at 2θ of 37.3°, 43.3°, and 62.9° were assigned to NiO. When XRD characteristic peak of the samples showed a weak and broad peak of NiO species, it actually indicated that NiO particles were very small and widely dispersed on the catalyst support [19]. Notably, the catalyst supported on α-Al_2O_3 showed the smallest NiO crystallite size among the tested catalysts, as shown in Table I. The reason might be that NiO well dispersed on the support, suppressing its aggregation.

H_2-TPR profiles of catalyst are shown in Fig.2(a). The peaks positioned at lower reduction temperature

DOI:10.1063/1674-0068/29/cjcp1603062

TABLE I Parameters of the catalysts.

Catalyst	$S_{BET}/(m^2/g)$	$V_{total}/(cm^3/g)$	D_p/nm	D_m/nm	NiO size/nm
Ni/α-Al_2O_3	172.9	0.316	7.3	3.9	11.4
Ni/γ-Al_2O_3	133.3	0.662	19.9	17.1	30.2
Ni/SiO_2	213.1	1.131	21.2	17.2	17.2
Ni/TiO_2	13.1	0.094	28.6	59.0	21.5
Ni/ZrO_2	34.2	0.153	17.9	17.0	17.8

Note: D_p is average pore diameter. D_m is the most probable pore diameter. NiO size is the size of NiO crystallite and calculated by Scherrer equation, the Bragg angle of 2θ was ~43.3°.

TABLE II Ni dispersion and H_2 uptakes of different catalysts.

Catalysts	H_2 uptaking/(μmol/g)	Ni dispersion/%
Ni/α-Al_2O_3	976.33	13.50
Ni/γ-Al_2O_3	459.72	6.36
Ni/SiO_2	566.95	7.84
Ni/TiO_2	201.86	2.79
Ni/ZrO_2	498.57	6.90

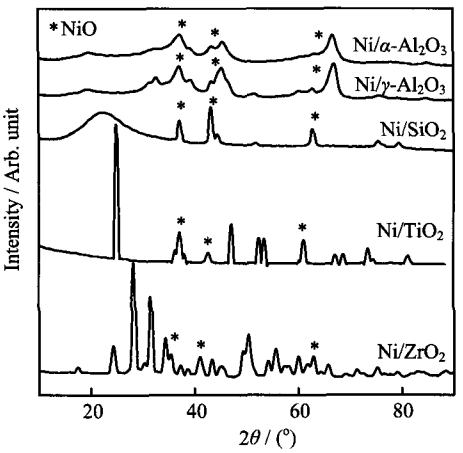

FIG. 1 XRD profiles of different catalysts.

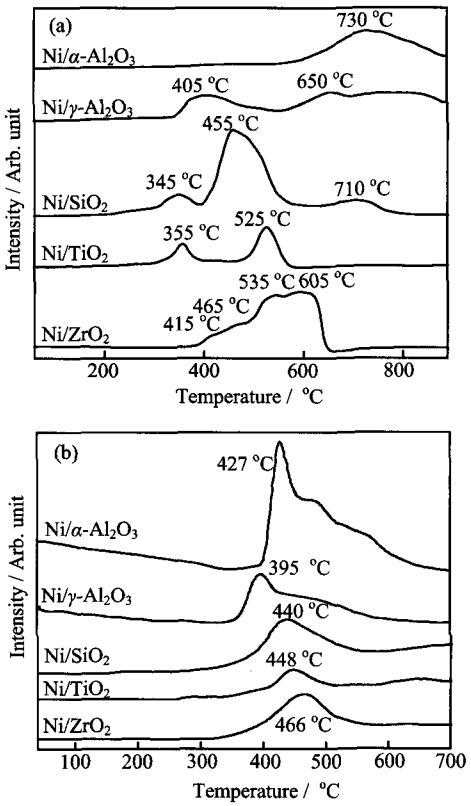

FIG. 2 (a) H_2-TPR and (b) H_2-TPD profiles of different catalyst samples.

(usually below 400 °C) were ascribed to the superficial NiO, which can be easily reduced to Ni^0. The peaks at higher temperature were associated with the reduction of bulk NiO, which weakly interacted with support material. It is noteworthy that the reduction peak of Ni/α-Al_2O_3 was centered at 730 °C, suggesting a stronger interaction between NiO and the support [20].

H_2-TPD experiments of different catalysts were also carried out, and the results are shown in Fig.2(b). H_2 desorption peaks stepped from about 320 °C for all investigated catalysts. The quantitative determination based on the H_2-TPD profiles demonstrated that the H_2 uptakes of Ni/α-Al_2O_3 (976.33 μmol/g) were far more than that of the Ni-based catalysts supported on γ-Al_2O_3, SiO_2, ZrO_2, and TiO_2 (as shown in Table II). In addition, Ni dispersion degree of Ni/α-Al_2O_3 (13.5%) was also higher than that of other tested catalysts. This conclusion is in good agreement with that of XRD analysis.

NH_3-TPD experiment was carried out to investigate the acidity of the catalyst. It is widely accepted that peaks at a temperature range of 100–400 °C are assigned to desorption of NH_3 on weak acidic sites and that peaks at a temperature range of 400–600 °C are assigned to the desorption of NH_3 on strong acidic sites. As shown in Fig.3, a NH_3 desorption band was observed in the pattern of Ni/α-Al_2O_3, suggesting the presence of acidic sites. Normally, α-Al_2O_3 is an in-

DOI:10.1063/1674-0068/29/cjcp1603062

TABLE III Anisole conversions and product yields over different catalysts.

Catalyst	Anisole conv./%	Yield/%				
		Hydrocarbons	Methoxy-cyclohexane	Cyclohexanol	Phenol	*o*-Cresol
Ni/α-Al_2O_3	93.25	90.47	0.81	0.63	0.92	0.31
Ni/γ-Al_2O_3	99.62	73.83	0.53	0	20.83	1.27
Ni/SiO_2	99.40	71.98	0	0.16	17.27	0
Ni/TiO_2	77.95	56.13	0	4.97	15.39	0
Ni/ZrO_2	93.52	62.02	0.32	0	25.91	2.88
α-Al_2O_3	10.33	1.47	0	0.16	6.65	0.97

TABLE IV Different hydrocarbons yields (%) over different catalysts.

Catalyst	Methylpentane	Cyclohexane	Cyclohexene	Methylcyclohexane	Toluene	Phenylcyclohexane
Ni/α-Al_2O_3	0.15	90.02	0.17	0	0	0.13
Ni/γ-Al_2O_3	0.69	50.83	4.13	2.11	15.91	0.16
Ni/SiO_2	0.94	66.24	2.34	0	2.46	0
Ni/TiO_2	0.24	54.83	0.35	0.58	0	0.13
Ni/ZrO_2	0.79	57.37	1.60	0.34	1.74	0.18
α-Al_2O_3	0	0.67	0.24	0	0.56	0

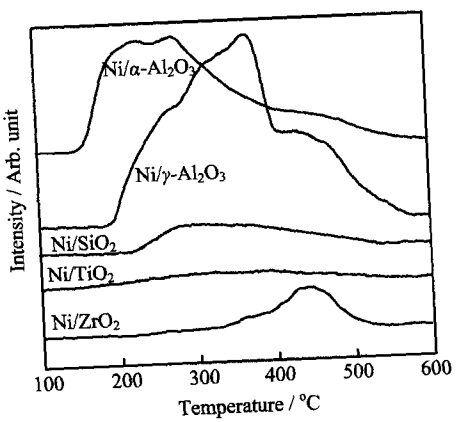

FIG. 3 NH_3-TPD profiles of the different catalyst samples.

ertial material. Detected acidic sites were deemed to be created by the introduction of Ni^{2+} cation [20]. It has been reported that trace Ni could be incorporated into α-Al_2O_3 through ion exchange [20]. A broad NH_3 desorption band was also observed as expected in the pattern of Ni/γ-Al_2O_3 catalyst. Compared with that of Ni/α-Al_2O_3, NH_3 desorption peak of Ni/γ-Al_2O_3 moved to higher temperature, suggesting stronger acidity. With regard to catalysts of Ni/SiO_2 and Ni/ZrO_2, relatively small peaks of NH_3 desorption were observed, suggesting a small amount of acidic sites. Notably, no NH_3 desorption peak was observed in the case of Ni/TiO_2.

B. Catalyst testing

Catalytic performances of catalysts and pure support α-Al_2O_3 were evaluated in HDO reaction process with anisole as substrate. As shown in Table III, the highest yield of hydrocarbons (90.47%) was obtained over Ni/α-Al_2O_3 catalyst. Cyclohexane was the main component, and its yield was as high as 90.02% (Table IV). This result indicates that the catalytic performance of α-Al_2O_3 was obviously superior to other catalysts under the same reaction conditions. This can be explained as: H_2 uptake of Ni/α-Al_2O_3 was obviously higher than that of other catalysts as discussed in H_2-TPD analysis suggesting more active nickel, thereby causing a better catalytic activity for hydrogenation. In addition, large number of acidic sites were observed on the surface of Ni/α-Al_2O_3. These acidic sites could co-work well together with active metal sites, and facilitate the HDO reaction [21]. However, the yield of hydrocarbon was rather low (1.47%) when pure support α-Al_2O_3 was used as catalyst, suggesting a negligible catalytic activity for the HDO reaction.

The conversion of anisole was as high as 99.62% over the catalyst Ni/γ-Al_2O_3. The major reason is the strong acidity of catalyst favors activation of the C–O bond, resulting in the cleavage of $C_{Ar}O-CH_3$ bond [2 It was reported that the phenolic compounds could al be converted over the support of γ-Al_2O_3 alone [2 However, compared with that of Ni/α-Al_2O_3 cataly the yield of hydrocarbon products was relatively l (only 73.83%). One of the reasons was ascribed to inefficient hydrogenation activity. For similar reas the hydrocarbon yields over Ni/SiO_2 and Ni/ZrO_2 w also relatively low.

It should be noted that the yield of toluene (Table was 15.91% over the catalyst Ni/γ-Al_2O_3. This also relate to the acidity of the catalyst. Norma anisole molecule can be adsorbed on the acidic due to its well accessible basic oxygen electronic

DOI:10.1063/1674-0068/29/cjcp1603062

blet, resulting in the activation of $ArO-CH_3$ bond. The activated $ArO-CH_3$ bond cleaved heterolytically, and the positively charged methyl group can be transferred to aromatic ring, leading to the formation of methylated products [24]. Therefore, it is plausible that the catalyst Ni/γ-Al_2O_3 favors the transmethylation due to its strong acidity, yielding higher methylated products during the HDO process of anisole. Similarly, methylated products were also observed over catalysts of Ni/SiO_2 and Ni/ZrO_2, although it was minor.

In addition, anisole conversion and hydrocarbon yield were relatively poor over the catalyst Ni/TiO_2. There are two possible reasons accounting for this. Firstly, H_2 uptake of Ni/TiO_2 is far less than that of other catalysts as discussed in H_2-TPD experiments, suggesting less active nickel. Moreover, the acidity of Ni/TiO_2 is almost negligible as discussed in NH_3-TPD experiments. Two handicaps resulted in an inferior catalytic activity for HDO reaction. Secondly, the BET surface area, Ni dispersion and porous structure of Ni/TiO_2 are clearly inferior to those of other investigated catalysts, which are also unfavorable for the improvement of catalytic activity.

Effects of reaction temperature, time and catalyst dosage on HDO of anisole were investigated carefully using Ni/α-Al_2O_3 as a representative catalyst. As shown in Fig.4(a), the anisole conversion gradually increased with the increased temperature. The yield of hydrocarbons also increased gradually from 38.90% to 90.47% when the reaction temperature increased from 220 °C to 300 °C. However, yield of hydrocarbons swiftly decreased as the reaction temperature further increased from 300 °C to 340 °C. In addition, bicyclic compound (phenylcyclohexane) noticeably increased in the products at 340 °C, suggesting that the intermolecular polymerization took place at a higher temperature. Detailed product distribution was presented in Table S1 (supplementary materials).

Reaction time significantly influenced the HDO reaction of anisole. As shown in Fig.4(b) and Table S2 (supplementary material), the conversion of anisole and the yield of hydrocarbons gradually increased with reaction time over Ni/α-Al_2O_3. At the beginning of the reaction, the yield of phenol is considerably high, and gradually reduced with reaction time being lengthened. According to this result, it can be speculated that anisole was converted to phenol via demethylation firstly, followed by hydrogenation of aromatic ring to form cyclohexanol and then cyclohexane. The detected cyclohexanol and cyclohexene were other evidences for this presumption. Interestingly, methoxycyclohexane was detected in the products obtained over Ni/α-Al_2O_3, suggesting that hydrogenation of the aromatic ring of anisole could occur prior to the demethylation. Generally, methoxycyclohexane was only mentioned as a reaction intermediate or product over noble metal catalyst due to its efficient hydrogenation activity [25].

The effect of catalyst dosage on the HDO of anisole

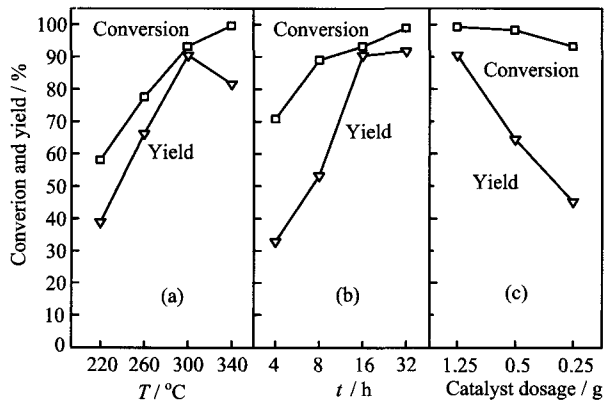

FIG. 4 Anisole conversion and hydrocarbon yield varied with (a) temperature, (b) time, and (c) catalyst dosage over Ni/α-Al_2O_3 catalyst. Reaction conditions: (a) catalyst of 0.5 g, anisole of 2.5 g, octane of 21.5 mL, P_{H_2}=5.0 MPa, t=16 h; (b) catalyst of 0.5 g, anisole of 2.5 g, octane of 21.5 mL, P_{H_2}=5.0 MPa, T=300 °C; (c) anisole of 2.5 g, octane of 21.5 mL, P_{H_2}=5.0 MPa, T=300 °C, t=16 h.

was also investigated in detail. As shown in Fig.4(c), the anisole conversion and the hydrocarbons yield gradually increased with the increased catalyst dosage in the investigated range. Generally, higher catalyst dosage implies more catalytic active sites, thereby resulting in better catalytic performance [26]. Therefore, it is plausible that this process is of high catalyst dosage dependence.

The repeatability of Ni/α-Al_2O_3 was also tested. The catalyst was reused directly without any retexture (such as calcination and reduction). As shown in Fig.5(a), anisole was efficiently converted with high hydrocarbons yield when the catalyst Ni/α-Al_2O_3 was repeatedly used. This result implied that the catalyst Ni/α-Al_2O_3 had a stable catalytic activity for the HDO of anisole. To examine the extent of coke formed during the HDO process, TG analysis of reused catalyst was carried out and the result was exhibited in Fig.S3 (supplementary materials). Only a slight weight loss was observed even if the catalyst was repeatedly reused for five times. This result suggests that the catalyst Ni/α-Al_2O_3 possesses excellent resistance to coking. However, as shown in the XPS patterns of catalysts (Fig.5(b)), the peak of Ni^0 positioned at 852.54 eV became small when the catalyst was repeatedly used for five times. Conversely, the peak of Ni^{2+} positioned at about 856 eV intensified obviously. This result suggests that active metal Ni^0 would be oxidized to Ni^{2+} during the HDO process of anisole.

IV. CONCLUSION

Effects of support materials α-Al_2O_3, γ-Al_2O_3, SiO_2, TiO_2, and ZrO_2 on catalytic performance of Ni-based catalysts were studied for the HDO of anisole to hydro-

DOI:10.1063/1674-0068/29/cjcp1603062

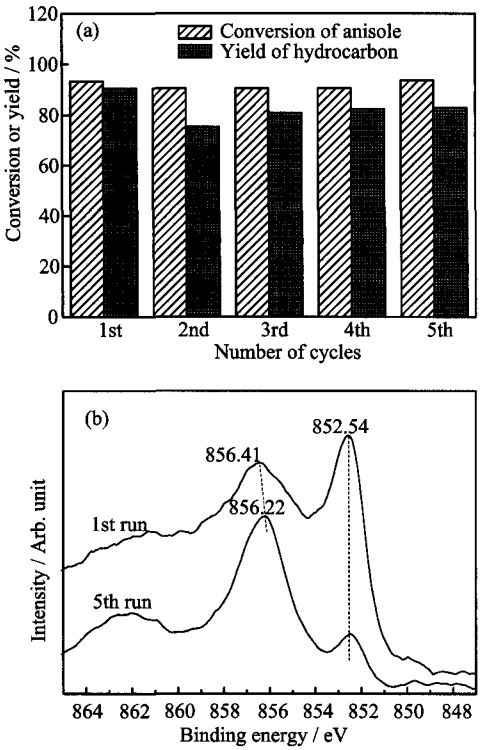

FIG. 5 (a) Catalyst repeatability test and (b) surface chemical state of catalysts. Reaction conditions: catalyst Ni/α-Al_2O_3 of 0.5 g, anisole of 2.5 g, octane of 21.5 mL, P_{H_2}=5.0 MPa, T=300 °C, and t=16 h.

carbons. The Ni/α-Al_2O_3 catalyst exhibited the most H_2 uptakes and the highest catalytic activity among these investigated catalysts, revealing that the higher hydrogenation activity can promote the HDO of anisole, obtaining higher hydrocarbon yield. Furthermore, the Ni/α-Al_2O_3 catalyst exhibited excellent repeatability for the HDO of anisole. However, the result of XPS analysis of the used catalyst demonstrated that active metal Ni^0 was oxidized to Ni^{2+} during the HDO process of anisole when the catalyst was repeatedly used for five times.

Supplementary materials: Table S1 and S2 show the conversion of anisole and product distribution varied with temperature and time, respectively. Figure S1 shows the pore size distribution of the different catalysts. Figure S2 shows the TEM image of Ni/α-Al_2O_3 catalyst. Figure S3 shows the TG curves of Ni/α-Al_2O_3 used in the first and the fifth run.

V. ACKNOWLEDGMENTS

This work was supported by the National Natural Science Foundation of China (No.51576198), the National Key Technology R&D Program (No.2014BAD02B01), and the Youth Innovation Promotion Association of Chinese Academy of Sciences (No.2015288).

[1] M. T. Klein and P. S. Virk, Energy Fuels. **22**, 2175 (2008).
[2] X. Li, J. Xing, M. Zhou, H. Zhang, H. Huang, C. Zhang, L. Song, and X. Li, Catal. Commun. **56**, 123 (2014).
[3] J. Zakzeski, P. C. A. Bruijnincx, A. L. Jongerius, and B. M. Weckhuysen, Chem. Rev. **110**, 3552 (2010).
[4] E. L. Kunkes, D. A. Simonetti, R. M. West, J. C. Serrano-Ruiz, C. A. Gartner, and J. A. Dumesic, Science **322**, 417 (2008).
[5] J. X. Long, Y. Xu, T. J. Wang, Z. Q. Yuan, R. Y. Shu, Q. Zhang, and L. Ma, Appl. Energ. **141**, 70 (2015).
[6] J. X. Long, Q. Zhang, T. J. Wang, X. H. Zhang, Y. Xu, and L. L. Ma, Bioresour. Technol. **154**, 10 (2014).
[7] J. X. Long, L. F. Wang, B. L. Yin, and X. H. Li, Chem. Eng. Sci. **122**, 24 (2015).
[8] X. H. Zhang, Q. Zhang, L. A. Chen, Y. Xu, T. J. Wang, and L. L. Ma, Chin. J. Catal. **35**, 302 (2014).
[9] C. Zhao, Y. Kou, A. A. Lemonidou, X. Li, and J. A. Lercher, Angew. Chem. Int. Ed. **48**, 3987 (2009).
[10] X. H. Zhang, Q. Zhang, T. J. Wang, L. L. Ma, Y. X. Yu, and L. G. Chen, Bioresour. Technol. **134**, 73 (2013).
[11] C. Zhao and J. A. Lercher, ChemCatChem. **4**, 64 (2012).
[12] G. Yao, G. J. Wu, W. L. Dai, N. J. Guan, and L. D. Li, Fuel **150**, 175 (2015).
[13] Y. Q. Yang, H. Luo, G. S. Tong, J. S. Kevin, and C. T. Tye, Chin. J. Chem. Eng. **16**, 733 (2008).
[14] Y. K. Hong, D. W. Lee, H. J. Eom, and K. Y. Lee, Appl. Catal. B **150**, 438 (2014).
[15] V. N. Bui, D. Laurenti, P. Delichere, and C. Geantet, Appl. Catal. B **101**, 246 (2011).
[16] E. Laurent and B. Delmon, J. Catal. **146**, 281 (1994).
[17] L. Nie and D. E. Resasco, J. Catal. **317**, 22 (2014).
[18] Z. C. Xie, Y. Wang, P. Wang, and L. Zhang, Appl. Mech. Mater. **33**, 513 (2014).
[19] S. B. Qiu, X. Zhang, Q. Y. Liu, T. J. Wang, Q. Zhang, and L. L. Ma, Catal. Commun. **42**, 73 (2013).
[20] T. M. Sankaranarayanan, A. Berenguer, C. Ochoa-Hernandez, I. Moreno, P. Jana, J. M. Coronado, D. P. Serrano, and P. Pizarro, Catal. Today **243**, 163 (2015).
[21] E. Díaz, A. F. Mohedano, L. Calvo, M. A. Gilarranz, J. A. Casas, and J. J. Rodríguez, Chem. Eng. J. **131**, 65 (2007).
[22] P. M. de Souza, R. C. Rabelo-Neto, L. E. P. Borges, G. Jacobs, B. H. Davis, T. Sooknoi, D. E. Resasco, and F. B. Noronha, Acs Catal. **5**, 1318 (2015).
[23] E. Laurent and B. Delmon, Appl. Catal. A **109**, 77 (1994).
[24] A. A. Dwiannoko, S. Lee, H. C. Ham, J. W. Choi, D. J. Suh, and J. M. Ha, Acs Catal. **5**, 433 (2015).
[25] G. Yuan, J. L. Lopez, C. Louis, L. Delannoy, and M. A. Keane, Catal. Commun. **6**, 555 (2005).
[26] J. Long, R. Shu, Z. Yuan, T. Wang, Y. Xu, X. Zhang, Q. Zhang, and L. Ma, Appl. Energ. **157**, 540 (2015).

DOI:10.1063/1674-0068/29/cjcp1603062